DOI: 10.3901/CJME.2014.01.032, available online at www.springerlink.com; www.cjmenet.com; www.cjmenet.com.cn

Mathematical Model and Experiment Validation of Fluid Torque by Shear Stress under Influence of Fluid Temperature in Hydro-viscous Clutch

CUI Hongwei[1], YAO Shouwen[1, 2, *], YAN Qingdong[1, 2], FENG Shanshan[1], and LIU Qian[1]

1 *School of Mechanical Engineering, Beijing Institute of Technology, Beijing 100081, China*
2 *National Key Laboratory of Vehicular Transmission, Beijing Institute of Technology, Beijing 100081, China*

Received March 13, 2013; revised August 8, 2013; accepted September 11, 2013

Abstract: The current design of hydro-viscous clutch(HVC) in tracked vehicle fan transmission mainly focuses on high-speed and high power. However, the fluid torque under the influence of fluid temperature can not be predicted accurately by conventional mathematical model or experimental research. In order to validate the fluid torque of HVC by taking the viscosity-temperature characteristic of fluid into account, the test rig is designed. The outlet oil temperature is measured and fitted with different rotation speed, oil film thickness, oil flow rate, and inlet oil temperature. Meanwhile, the film torque can be obtained. Based on Navier-Stokes equations and the continuity equation, the mathematical model of fluid torque is proposed in cylindrical coordinate. Iterative method is employed to solve the equations. The radial and tangential speed distribution, radial pressure distribution and theoretical flow rate are determined and analyzed. The models of equivalent radius and fluid torque of friction pairs are introduced. The experimental and theoretical results indicate that tangential speed distribution is mainly determined by the relative rotating speed between the friction plate and the separator disc. However, the radial speed distribution and pressure distribution are dominated by pressure difference at the lower rotating speed. The oil film fills the clearance and the film torque increases with increasing rotating speed. However, when the speed reaches a certain value, the centrifugal force will play an important role on the fluid distribution. The pressure is negative at the outer radius when inlet flow rate is less than theoretical flow, so the film starts to shrink which decreases the film torque sharply. The theoretical fluid torque has good agreement with the experimental data. This research proposes a new fluid torque mathematical model which may predict the film torque under the influence of temperature more accurately.

Keywords: hydro-viscous clutch, fluid torque by shear stress, experiment validation, mathematical model

1 Introduction

In order to keep the power transmission system of tracked vehicles in suitable condition, 12 to 14 percent of engine power will be consumed by fans, which reduce the output power greatly[1]. The hydro-viscous clutch(HVC) is a new kind of fan transmission which can realize step-less speed regulating and play an important role in energy-saving[2].

The HVC, also called the Omega clutch, consists of a series of separator discs and friction plates, input axis, output axis and viscous fluid. The friction-lining materials are bonded to the core disks of friction plates[3]. Usually, the input rotation speed of HVC is constant. The torque will be generated by the relative rotation between the friction plates and the separator discs. Meanwhile, the output speed is changed by changing the thickness of oil film through a clutch piston which is acted on by control oil. There are three stages of speed regulation. The first stage is fluid transmission caused by shear stress. The second stage is mixed lubrication, where the surface asperities come into contact as the fluid film thickness is decreasing. The third stage is boundary lubrication when the two surfaces come into contact until the relative velocity becomes zero[4–5].

At present, the fluid torque by shear stress is still calculated based on Newton's law of viscosity with assumptions of full film and laminar flow between friction plates and separator discs. The flow between two rotating plates has been extensively studied both by theoretical models and experiments[6–9]. HASHIMOTO, et al[10], gave the governing equations for turbulent flow and considered the centrifugal effect in the thrust bearing. KATO, et al[11] utilized the equations provided by Hashimoto to derive the film pressure distribution and the film torque of disengaged wet clutch. YUAN, et al[12], thought that the surface tension force was the main reason in retaining the oil film in clutch clearances. An equivalent radius assumption was introduced to facilitate the inclusion of surface tension where the full oil started to shrink due to the centrifugal effects. Their prediction model can verify the test result quite well. However, errors still remain largely for those rotations beyond the peak torque region.

* Corresponding author. E-mail: yshouwen@gmail.com
This project is supported by National Natural Science Foundation of China (Grant No. 51275039)

YUAN, et al[13], developed a gas-liquid two-phase flow model to study the film torque by using the computational fluid dynamics software FLUENT, where the volume of fluid (VOF) technique proposed by HIRT, et al[14] was used. The discrepancy is that the film torque will decrease sharply to nearly zero. HU, et al[15] estimated the film area by the equivalent circumferences caused by pressure difference, film centrifugal force and inertia force. YUAN, et al[16] formulated a film torque with a consideration of centrifugal force and validated it through test data. The result of test is not true, especially at higher rotational speeds.

During the slipping of HVC or engagement of the wet clutch, a large amount of heat is generated. To provide more effective cooling, many groove patterns are designed on the friction facings to facilitate the flow across the faces[17−18]. It is difficult to derive mathematical model with the consideration of groove effects. The experimental tests are effective methods to study the factors of grooves and surface tension. HU, et al[19], set up a small experimental rig to test a grooved single-plate wet clutch and verify the effects of the clearance, rotating speed, groove depth and friction material for declining, screw, and radial grooves. However, this method cannot be used to predict the film torque yet.

For the consideration of grooves, apart from the literatures mentioned above, RAZZAQUE, et al[20], studied the groove of friction plates during the engagement period and analyzed the torque characteristics. APHALE, et al[21], developed a 2D lubrication model and a 3D computational fluid dynamics(CFD) model with the consideration of grooved plates to evaluate the film torque. However, the film torque is quite different between the mathematical model and the experimental data.

From the above review of the previous work, the film torque results are quite different from the experimental data especially when the friction plate is rotating at high speeds. Besides, test results show that the oil temperature has a tremendous effect on the film torque. But the influences of fluid temperature and viscosity-temperature characteristic on fluid torque are not considered in most calculations. Therefore, the objective is to introduce this important factor into the film torque prediction model for HVC, and validate the theory through test data. The mathematical model of fluid torque caused by shear stress was derived in cylindrical coordinate by taking the viscosity-temperature characteristic of the fluid into account. The radial speed distribution, tangential speed distribution, pressure distribution and theoretical flow rate were solved by iterative method. The model of equivalent radius was created and fluid torque of friction pairs was calculated. The results show that the theoretical data has good agreement with the experimental data, which means that the film torque can be predicted more accurately by the models.

2 Experiment of Fluid Torque and Analysis of the Oil Temperature

2.1 Test rig

The test rig is shown in Fig. 1, which is used to measure the torque, rotating speed, fluid pressure, and temperature of the HVC. The test rig is comprised of an inverter-type motor, gear case, HVC, eddy current dynamometer, torque-speed transducers, thermocouples, pressure gauges, and flow meter.

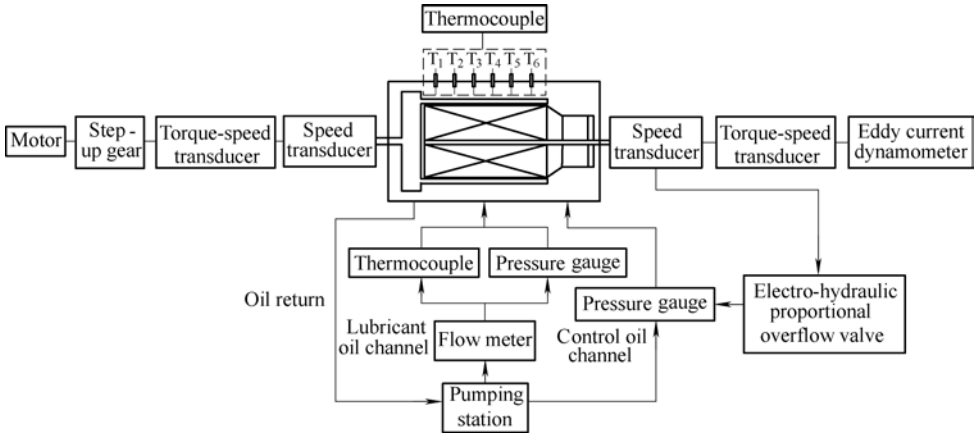

Fig. 1. Test rig of film torque of HVC

The friction plates are driven by the motor, and the rotational speed is increased by one stage gear case with the speed ratio of 0.5. The separator discs are loaded by the eddy current dynamometer which is driven by the shear stress of the fluid. The rotational speed and torque may be obtained by the torque-speed transducer in different conditions by adjusting the control oil. The torque can be regarded as the fluid torque caused by shear stress approximately. Meanwhile, the flow rate of oil and inlet oil temperature can be measured by the flow meter and thermocouple respectively.

The inlet lubricant oil is pumped by the motor through a flow meter. One thermocouple monitors the oil temperature as it enters the clutch. Six thermocouples, which are evenly distributed along the axial direction of the outlet, are used to measure the oil temperature when it is ejected from the

outer radius.

The geometric parameters are listed in Table 1. The properties of fluid, 15W-40, are listed in Table 2.

Table 1. Geometric parameters of friction pair

Geometric parameter	Value
Outer diameter R_2/mm	123
Inner diameter R_1/mm	86
Rotation of friction plates ω_1/(r • min^{-1})	0–4 200
Rotation of separator discs ω_2/(r • min^{-1})	0–ω_1
Oil film thickness h/mm	0.1–0.3
Number of friction pairs N	24

Table 2. Properties of oil

Oil properties	Value
Flow rate q/(L • min^{-1})	20–60
Density ρ/(kg • m^{-3})	886
Pressure of inlet p_0/MPa	0.3
Temperature of inlet t_{in}/℃	25–75

2.2 Analysis and fitting of the outlet oil temperature

The average value of the data from the six thermocouples can be considered as outlet oil temperature. The outlet oil temperature t_{out} were measured at different relative rotational speed $\omega_1-\omega_2$, different oil film thickness h, different flow rate of oil q and different inlet oil temperature t_{in}. After normalization, the outlet oil temperature can be obtained in different conditions.

In iSIGHT, the relative rotational speed, oil film thickness, flow rate of oil and inlet oil temperature were considered as variables and outlet oil temperature was considered as an output. The main effect of each parameter on the outlet oil temperature can be obtained by design of experiment technology, which is shown in Fig. 2.

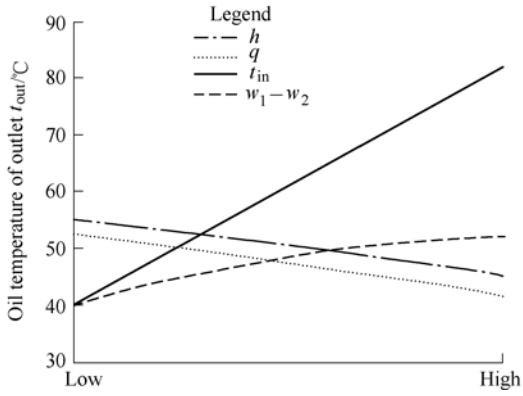

Fig. 2. Main effect of each parameter on outlet oil temperature

As may be seen, the outlet oil temperature increases monotonously with increasing relative rotational speed and inlet oil temperature. Meanwhile, the inlet oil temperature has a greater influence on outlet oil temperature. The outlet oil temperature has an inverse relationship with the oil film thickness and flow rate.

The experiment data can be fitted by the response surface method. By error analysis, the quartic response surface fitting has higher accuracy. The approximate expression of outlet oil temperature is shown as follows:

$$\begin{aligned} t_{out} = &-215.37-447.18q+1\,273.99t_{in}-1.71(\omega_1-\omega_2)+\\ &158.23h+727.95q^2-1936.43t_{in}^2+16.35(\omega_1-\omega_2)^2-\\ &261.19h^2+53.68qt_{in}+0.63q\cdot(\omega_1-\omega_2)-10.22qh+\\ &8.38t_{in}(\omega_1-\omega_2)+0.75t_{in}h-2.88(\omega_1-\omega_2)h-\\ &528.42q^3+1242.65t_{in}^3-10.2(\omega_1-\omega_2)^3+190.67h^3+\\ &137.66q^4-290.82t_{in}^4+1.85(\omega_1-\omega_2)^4-49.57h^4. \end{aligned} \quad (1)$$

3 Mathematical Model

The single friction pair is simplified at the fluid transmission stage of the HVC. Cylindrical coordinate is used to describe the principle of film torque, as shown in Fig. 3.

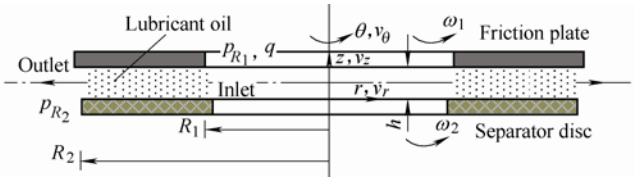

Fig. 3. Schematic model of film torque in cylinder coordinates

r, z, θ —Radial, axial and tangential coordinate
v_r, v_z, v_θ —Radial, axial and tangential velocity component
P_{R_1}, P_{R_2}—Inlet pressure and outlet pressure

The following assumptions are made to simplify the model: 1) the fluid is an incompressible Newtonian fluid, so that the density ρ is constant; 2) the lubricant flow is laminar between the friction plate and separator disc (Reynolds number Re is 130, which is less than the threshold); 3) the flow is axisymmetric, $\partial v_i/\partial\theta=0, i=r,\theta,z$; 4) the fluid speed is time-invariant, $\partial v_i/\partial t=0, i=r,\theta,z$; 5) the lubricant oil is no sliding on the face of the friction plate; 6) the gravity force is neglected, namely $F_r=F_\theta=F_z$=0; 7) the axial velocity is also neglected, $v_z=0$; 8) the friction plate is non-grooved; 9) the pressure gradient along the axial direction is zero, $\partial p/\partial z=0$; 10) the velocity gradient in the axial direction is greater than that of the radial direction, $\partial v_\theta/\partial z \gg \partial v_\theta/\partial r$, $\partial^2 v_\theta/\partial z^2 \gg \partial^2 v_\theta/\partial z\partial r \gg \partial^2 v_\theta/\partial r^2$, $\partial v_r/\partial z \gg \partial v_r/\partial r$, $\partial^2 v_r/\partial z^2 \gg \partial^2 v_r/\partial z\partial r \gg \partial^2 v_r/\partial r^2$;

With the hypothesis above, the Navier-Stokes equations can be written as Eq. (2):

$$\begin{cases} \dfrac{\partial p}{\partial r}-\rho\dfrac{v_\theta^2}{r}+\rho v_r\dfrac{\partial v_r}{\partial r}=\mu(t_{out})\left(\dfrac{\partial^2 v_r}{\partial z^2}-\dfrac{v_r}{r^2}+\dfrac{\partial^2 v_r}{\partial r^2}+\dfrac{1}{r}\dfrac{\partial v_r}{\partial r}\right),\\ \rho v_r\dfrac{\partial v_\theta}{\partial r}+\rho\dfrac{v_r v_\theta}{r}=\mu(t_{out})\left(\dfrac{1}{r}\dfrac{\partial v_\theta}{\partial r}-\dfrac{v_\theta}{r^2}+\dfrac{\partial^2 v_\theta}{\partial r^2}+\dfrac{\partial^2 v_\theta}{\partial z^2}\right),\\ \dfrac{\partial p}{\partial z}=0, \end{cases} \quad (2)$$

where p is the oil film pressure, $\mu(t_{\text{out}})$ is the dynamic viscosity of fluid.

The fluid continuity equation can also be simplified as

$$\frac{\partial v_r}{\partial r}+\frac{v_r}{r}=0\,. \tag{3}$$

To account for the fluid viscosity variation with temperature, the formula of the viscosity-temperature characteristic is given as follows:

$$\mu(t_{\text{out}})=\frac{\rho}{8.480\,96t_{\text{out}}^2-185.068t_{\text{out}}+3\,406.94}\,. \tag{4}$$

The boundary conditions are as follows:

$$\begin{cases} v_r(r,0)=v_r(r,h)=0, \\ v_\theta(r,0)=\omega_2 r, v_\theta(r,h)=\omega_1 r, \\ p_{R_2}=0, \\ p_{R_1}=p_0. \end{cases} \tag{5}$$

Eq. (2) can be expressed as an ordinary differential equation shown in Eq. (6):

$$\begin{cases} \dfrac{\mathrm{d}p}{\mathrm{d}r}-\dfrac{\rho}{r}(v_r^2+v_\theta^2)=\mu(t_{\text{out}})\dfrac{\mathrm{d}^2v_r}{\mathrm{d}z^2}, \\ 2\rho\dfrac{v_r v_\theta}{r}=\mu(t_{\text{out}})\dfrac{\mathrm{d}^2v_\theta}{\mathrm{d}z^2}. \end{cases} \tag{6}$$

Eq. (6) is a set of non-homogeneous ordinary differential equations. As left term of the equations has nonlinear expressions, an accurate analytical solution of the equations cannot be obtained. Therefore the equations were solved by using an iterative method. Firstly, the homogeneous equations can be derived and solved by neglecting the inertial expression. The analytical solutions of v_r' and v_θ' can then be solved. Secondly, the approximate analytical solution of v_r, v_θ, p and q can be acquired by using the results from the first step.

The homogeneous equations are as follows:

$$\begin{cases} \mu(t_{\text{out}})\dfrac{\mathrm{d}^2v_r}{\mathrm{d}z^2}-\dfrac{\mathrm{d}p}{\mathrm{d}r}=0, \\ \mu(t_{\text{out}})\dfrac{\mathrm{d}^2v_\theta}{\mathrm{d}z^2}=0. \end{cases} \tag{7}$$

By integration, the analytical solutions of v_r' and v_θ' can be obtained from the boundary conditions:

$$v_r'=\frac{1}{2\mu(t_{\text{out}})}\frac{\mathrm{d}p}{\mathrm{d}r}z(z-h)\,, \tag{8}$$

$$v_\theta'=\frac{(\omega_1-\omega_2)r}{h}z+\omega_2 r\,. \tag{9}$$

The theoretical flow rate q_i can be determined by integrating the radial velocity over the surface area:

$$q_i=2\pi r\int_0^h v_r'\mathrm{d}z\,, \tag{10}$$

where q_i is the flow rate that fill each clearance of friction pair.

Substituting Eq. (8) into Eq. (10), we get,

$$\frac{\mathrm{d}p}{\mathrm{d}r}=-\frac{6\mu(t_{\text{out}})q_i}{\pi r h^3}\,. \tag{11}$$

After substituting Eq. (11) into Eq. (8), then v_r' can be rewritten as

$$v_r'=\frac{3q_i z(h-z)}{\pi r h^3}\,. \tag{12}$$

Thus, the tangential velocity can be obtained as follows:

$$v_\theta=\frac{\rho q_i}{\mu(t_{\text{out}})\pi r h^3}\left[\omega_2 h z^3+\frac{1}{2}z^4(\omega_1-2\omega_2)-\frac{3(\omega_1-\omega_2)}{10h}z^5-\frac{zh^3(2\omega_1+3\omega_2)}{10}\right]+\frac{(\omega_1-\omega_2)rz}{h}+\omega_2 r. \tag{13}$$

Note that in Eq. (13), the tangential velocity is affected by the rotation of the friction plates, the rotation of the separator discs, and the inlet flow rate. The tangential velocity is composed of two parts. The first part is caused by flow inertia. The second part can be approximated as Couette flow. The velocity increases with the radius of the friction plate.

The radial velocity can be got as follows:

$$v_r=\frac{3\rho {q_i}^2 z}{20\mu(t_{\text{out}})\pi^2 r^3 h^6}(h^5-2z^5+6hz^4-5h^2z^3)+\frac{1}{2\mu(t_{\text{out}})}\frac{\mathrm{d}p}{\mathrm{d}r}(z^2-zh)+\frac{\rho rz}{12\mu(t_{\text{out}})h^2}\left[h^3(\omega_1^2+2\omega_1\omega_2+3\omega_2^2)-(\omega_1-\omega_2)^2z^3-4\omega_2(\omega_1-\omega_2)hz^2-6\omega_2^2h^2z\right]. \tag{14}$$

The theoretical flow rate can be obtained by integrating the radial velocity:

$$q_i=-\frac{r\pi h^3}{6\mu(t_{\text{out}})}\frac{\mathrm{d}p}{\mathrm{d}r}+\frac{9\rho {q_i}^2 h}{140\mu(t_{\text{out}})\pi r^2}+\frac{\pi\rho r^2h^3}{60\mu(t_{\text{out}})}(3\omega_1^2+4\omega_1\omega_2+3\omega_2^2) \tag{15}$$

Thus, we get the following:

$$\frac{\mathrm{d}p}{\mathrm{d}r}=\frac{27\rho {q_i}^2}{70\pi^2 r^3 h}+\frac{\rho r}{10}(3\omega_1^2+4\omega_1\omega_2+3\omega_2^2)-\frac{6\mu(t_{\text{out}})q_i}{r\pi h^3}\,. \tag{16}$$

Substituting Eq. (16) into Eq. (14), the radial velocity can be rewritten as

$$v_r = -\frac{3q_i}{r\pi h^3}(z^2 - zh) + \frac{\rho {q_i}^2}{140\pi^2 r^3 \mu(t_{\text{out}})h^6} \times (27h^4z^2 - 6zh^5 - 42z^6 + 126z^5h - 105z^4h^2) + \frac{\rho r z(\omega_1 - \omega_2)}{60\mu(t_{\text{out}})h^2}\left[3h^2z(3\omega_1 + 7\omega_2) - 2h^3(2\omega_1 + 3\omega_2) - 5z^3(\omega_1 - \omega_2) - 20hz^2\omega_2\right]. \quad (17)$$

Shown in Eq. (17), it is clear that the radial velocity is mainly affected by the rotation of the friction plates and separator discs, and the inlet flow rate. The expression for radial velocity can be divided into three parts. The first part is caused by the steady pressure difference between the inlet and outlet. The radial speed decreases with increasing radius, which shows a quadratic parabola and can be approximated as Poiseuille flow. The second part is caused by the inertia force, which is less than the other terms when the flow rate is low. The third part is the flow caused by the centrifugal force since the radial speed increases with the rotating speed.

Under specific boundary conditions, the pressure of the outer radius p_{R_2} is zero. The pressure distribution of the oil film can be obtained by the integration of Eq. (16) along the radial direction:

$$p(r) = \frac{6\mu(t_{\text{out}})q_i}{\pi h^3}\ln\frac{R_2}{r} + \frac{27\rho {q_i}^2}{140\pi^2 h^2}\left(\frac{1}{R_2^2} - \frac{1}{r^2}\right) + \frac{\rho}{20}(3\omega_1^2 + 4\omega_1\omega_2 + 3\omega_2^2)(r^2 - R_2^2). \quad (18)$$

In Eq. (18), the pressure is also mainly determined by the inlet flow rate and the rotating speed of friction pairs, and it also consists of three terms, namely the pressure difference, and the force of inertial and the centrifugal force. The first term makes the pressure positive and decreases in the radial direction from the inner radius to the outer radius. The second part can also be neglected. The third makes the pressure negative, and is versus to the first term in radial direction.

Substituting the pressure boundary $p_{R_1} = p_0$ into Eq. (18), the fluid pressure can be expressed as

$$p_0 = \frac{6\mu(t_{\text{out}})q_i}{\pi h^3}\ln\frac{R_2}{R_1} + \frac{27\rho q_i^2}{140\pi^2 h^2}\left(\frac{1}{R_2^2} - \frac{1}{R_1^2}\right) + \frac{\rho}{20}(3\omega_1^2 + 4\omega_1\omega_2 + 3\omega_2^2)(R_1^2 - R_2^2) \quad (19)$$

Solving Eq. (19), the flow rate between friction plate and separator disc is

$$q_i = \frac{\dfrac{6\mu(t_{\text{out}})}{\pi h^3}\ln\dfrac{R_2}{R_1} - \sqrt{\left[\dfrac{6\mu(t_{\text{out}})}{\pi h^3}\ln\dfrac{R_2}{R_1}\right]^2 - \dfrac{54}{70\pi^2h^2}\left(\dfrac{1}{R_1^2} - \dfrac{1}{R_2^2}\right)\left[\dfrac{\rho}{20}(3\omega_1^2 + 4\omega_1\omega_2 + 3\omega_2^2)(R_2^2 - R_1^2) + p_0\right]}}{\dfrac{27\rho}{70\pi^2h^2}\left(\dfrac{1}{R_1^2} - \dfrac{1}{R_2^2}\right)}. \quad (20)$$

The theoretical flow rate in Eq. (20), which can keep full oil film between the plate and disc, is proportional to the rotating speed of the friction plate. But in engineering applications, the feeding flow rate is usually constant. When the rotating speed is low, the centrifugal force and radial velocity are small. Meanwhile, the outlet pressure of friction pairs is positive. The feeding flow rate is greater than the theoretical, which indicates that the clearance is filled with oil. However, when the speed reaches a certain value, the centrifugal force becomes dominant and drives the fluid outward. As a result, the pressure becomes negative, which means the feeding flow rate is less than needed. Consequently, the film starts to shrink and a partial oil film occurs.

In order to predict the film torque by shear stress of HVC when the oil film starts to shrink at high-speed, an equivalent radius assumption is used. The outer radius of the hypothesized film is shown in Fig. 4. The film torque is only generated by the film area. Thus,

if $q \geqslant q_i$, then $R_0 = R_2$;

if $q < q_i$, then

$$\begin{cases} q_i = \pi h(R_2^2 - R_1^2), \\ q = \pi h(R_0^2 - R_1^2). \end{cases} \quad (21)$$

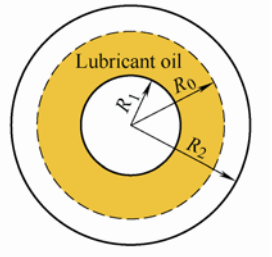

Fig. 4. Schematic of partial oil film with equivalent radius (R_0 is equivalent radius)

Solving Eq. (21), the film equivalent radius is

$$R_0 = \sqrt{\frac{q}{q_i}R_2^2 + \left(1 - \frac{q}{q_i}\right)R_1^2}. \quad (22)$$

The film shear torque is calculated according to the schematic model shown in Fig. 5.

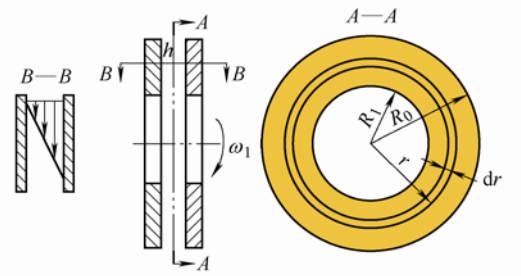

Fig. 5. Schematic of film torque model

The film shear stresses of friction plates and separator discs are calculated according to the Newton inner friction law.

The friction plates:

$$\tau_{\theta 1}(z=h)=\mu(t_{\text{out}})\left.\frac{\mathrm{d}v_\theta}{\mathrm{d}z}\right|_{z=h}= -\frac{\rho q_i}{\pi r}\left(\frac{27}{200}\omega_1+\frac{47}{300}\omega_2\right)+\frac{\mu(t_{\text{out}})(\omega_1-\omega_2)r}{h}; \tag{23}$$

The separator discs:

$$\tau_{\theta 2}(z=0)=\mu(t_{\text{out}})\left.\frac{\mathrm{d}v_\theta}{\mathrm{d}z}\right|_{z=0}= -\frac{\rho q_i}{10\pi r}(2\omega_1+3\omega_2)+\frac{\mu(t_{\text{out}})(\omega_1-\omega_2)r}{h}. \tag{24}$$

where $\tau_{\theta 1}$, $\tau_{\theta 2}$ are the film shear stresses of friction plates and separator discs.

Integrating from inner radius R_1 to outer radius R_0 of the oil film in radial direction, the film torques of friction plates and separator discs are shown as follows.

The friction plates:

$$T_1=2\pi N\int_{R_1}^{R_0}\tau_{\theta 1}r^2\mathrm{d}r=-\rho q_i N\left(\frac{27}{200}\omega_1+\frac{47}{300}\omega_2\right)(R_0^2-R_1^2)+\frac{\pi N\mu(t_{\text{out}})(\omega_1-\omega_2)}{2h}(R_0^4-R_1^4); \tag{25}$$

The separator discs:

$$T_2=2\pi N\int_{R_1}^{R_0}\tau_{\theta 2}r^2\mathrm{d}r=-\frac{1}{10}N\rho q_i(2\omega_1+3\omega_2)(R_0^2-R_1^2)+\frac{\pi N\mu(t_{\text{out}})(\omega_1-\omega_2)}{2h}(R_0^4-R_1^4). \tag{26}$$

where T_1, T_2 are the film torques of friction plates and separator discs.

As shown in Eq. (25) and Eq. (26), it is clear that the film torques of the friction plates and separator discs comprise two parts. The first part is the loss of torque resulting from the flow inertia, which has little influence on the total torque. The second part is the oil film shear torque generated by the relative rotation between the friction plates and separator discs, which plays an important role in the total torques of friction pairs. Meanwhile, from Eq. (25) and Eq. (26), the film torques of the friction plates and separator discs are unequal. The difference is $\Delta T=T_1-T_2$, which may be ignored because it is very small.

4 Film Torque Model Validation

The mathematical film torque model is validated based on experimental data. The output rotation speed is 0r/min. The film thickness is 0.3 mm. The inlet oil temperature is 30 ℃ and the flow rate is 20 L/min. The parameters of the friction pairs and lubricant oil are listed in Table 1 and Table 2 respectively.

Fig. 6–Fig. 8 illustrate the radial speed distribution caused by the pressure difference, the force of inertia and the centrifugal force, respectively. Fig. 9 shows the total radial speed distribution when input rotation speed is 2.5 kr/min. As shown, the radial speed distribution caused by pressure the difference decreases in the radial direction, which is similar to a parabola in the axial direction. The radial speed distribution caused by the centrifugal force will change from negative to positive in axial direction, where the parabolic profile can also be observed. The absolute value of the radial speed caused by the centrifugal force will increase in radial direction. The pressure difference has a dominant effect on the radial speed, while the centrifugal force effect is less. The force of inertia can be neglected.

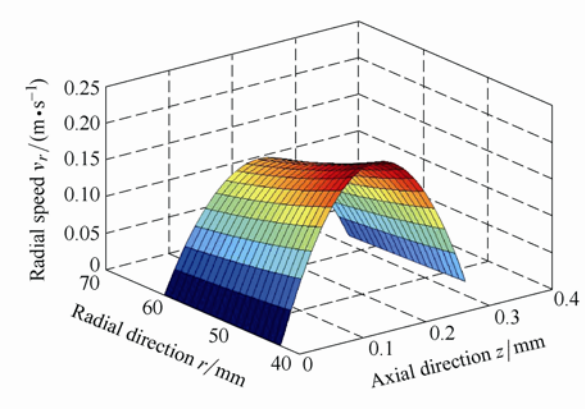

Fig. 6. Radial speed distribution caused by pressure difference

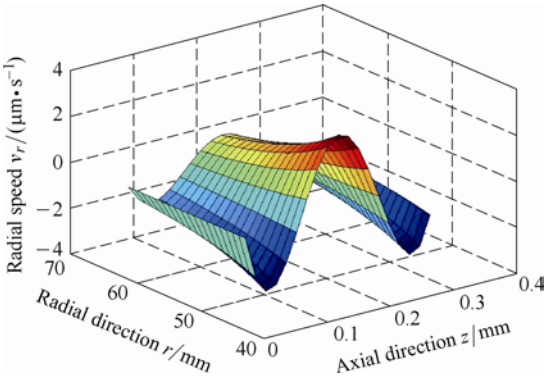

Fig. 7. Radial speed distribution caused by inertia

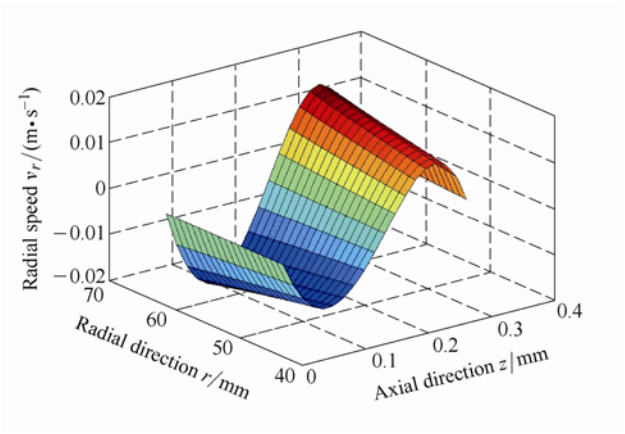

Fig. 8. Radial speed distribution caused by centrifugal force

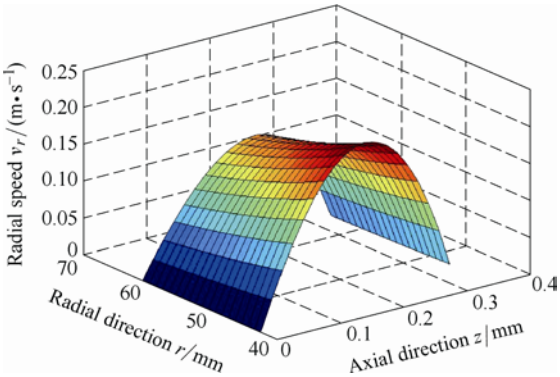

Fig. 9. Speed distribution in radial direction

Fig. 10–Fig. 11 show the tangential speed distribution caused by flow inertia and the relative rotation of friction pairs. Fig. 12 shows the total tangential speed distribution when the input rotation speed is 2.5 kr/min. Obviously, the tangential speed distribution caused by the flow inertia increases in the radial direction, and is similar to a parabola in the axial direction. But its contribution is very small that it may be ignored. Besides, the tangential speed distribution caused by the relative rotation of friction plates and separator discs increases in both the radial and axial directions.

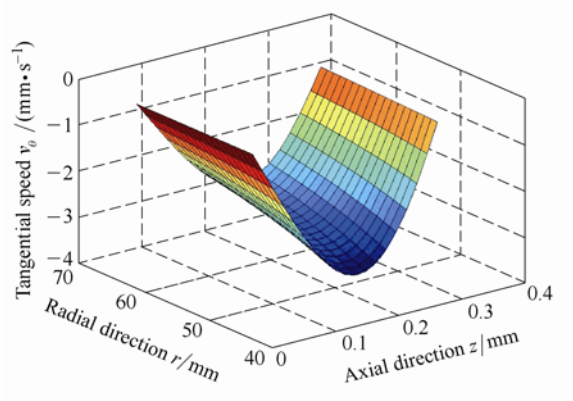

Fig. 10. Tangential speed distribution caused by the flow inertia

Fig. 13 and Fig. 14 show the pressure distribution when the input rotation speeds are 2.0 kr/min and 2.4 kr/min respectively. The pressure caused by the force of inertia can be neglected. The pressure, which is caused by the pressure difference, is positive, and decreases as the fluid approaches the outer radius. However, the pressure caused by centrifugal force become negative, and increases as the fluid moves outward. The pressure difference is the main factor of pressure at the speed of 2.0 kr/min, while the centrifugal force contributes more at 2.4 kr/min. Note that the total pressure is negative at the outer radius at 2.4 kr/min.

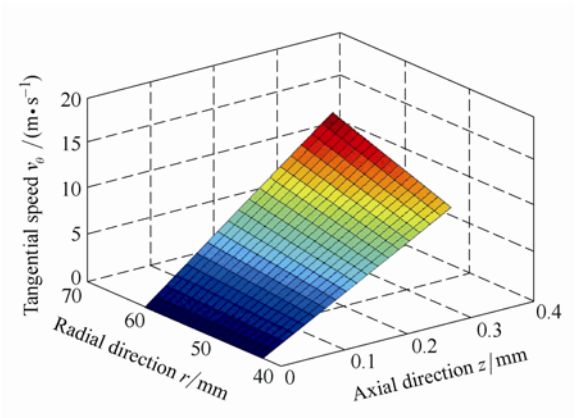

Fig. 11. Tangential speed distribution caused by relative rotation

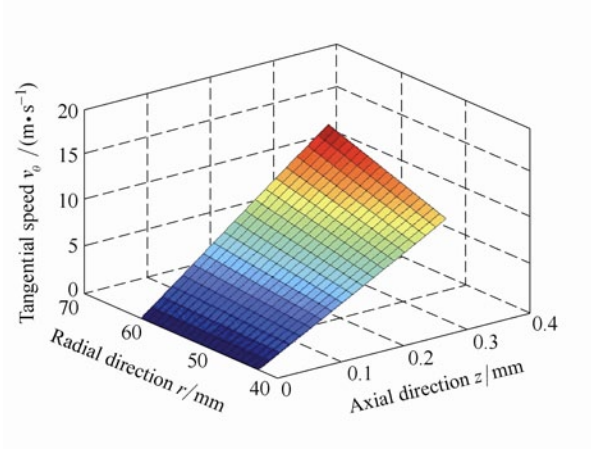

Fig. 12. Tangential speed distribution

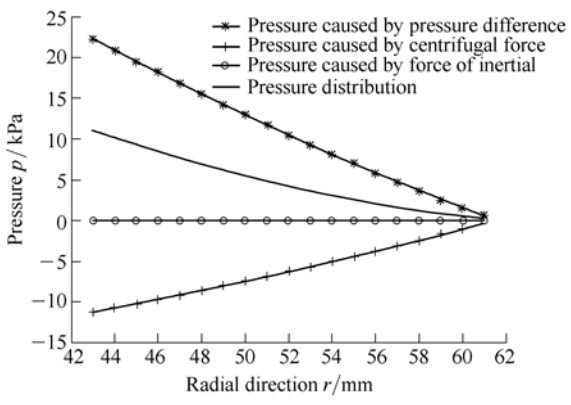

Fig. 13. Pressure distribution at 2.0k r/min

Fig. 15 shows the theoretical flow rate that is needed to

maintain a full oil film in the friction pairs, which increases as the rotating speed increases. When the rotating speed reaches 2.4 kr/min, the inlet flow, which is constant, is lower than the theoretical flow rate. The film begins to shrink, as shown in Fig. 4. The negative pressure is also verified at the outlet, as shown in Fig. 14.

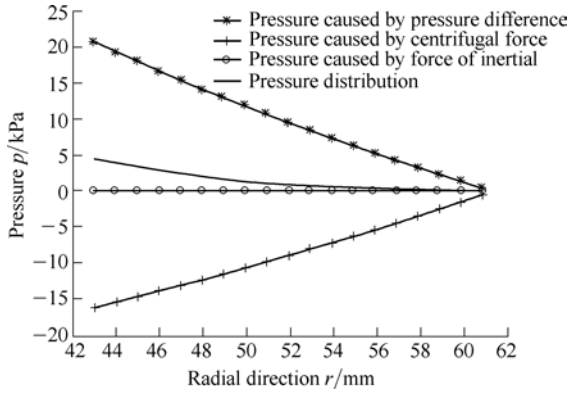

Fig. 14. Pressure distribution at 2.4k r/min

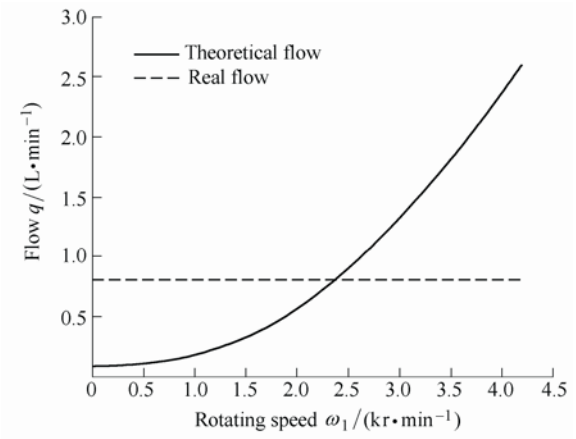

Fig. 15. Theoretical flow and inlet flow of HVC

The outer radius of the oil film predicted by the model with respect to the rotational speed of the friction plate is shown in Fig. 16. A full oil film between the plate and the disc exists until the speed reaches 2.4 kr/min, where the outer radius starts to drop sharply.

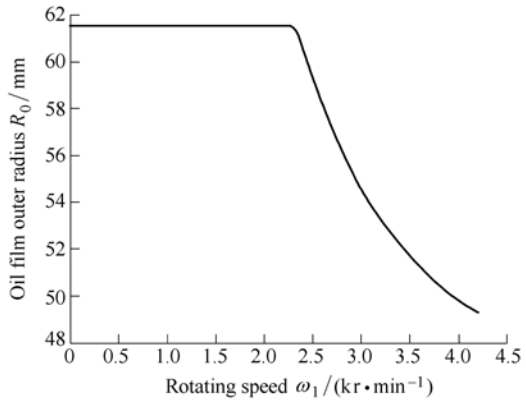

Fig. 16. Prediction of oil film outer radius

In the same condition, which is mentioned in the mathematical model, the fluid torque can be obtained by a torque-speed transducer at different rotating speeds in the test rig. Fig. 17 is the comparison of film torque between the theoretical model and test data, which shows that the prediction agrees with the test results fairly well in the whole range of clutch speed. The conclusions are as follows: as the increasing of relative rotational speed, the film torque increases monotonically but the trend is not linear. The reason is that the oil viscosity decreases because the temperature goes up as the rotating speed increases. When the rotating speed is 2.4 kr/min, the film torque reaches its peak and then begins to decrease sharply. An explanation of this phenomenon is insufficient flow in shrinking film area of the friction pair. The film outer radius has tremendous effect on the film torque. The theoretical data has perfect agreement with experimental data, which means that the torque model can predict the film torque correctly.

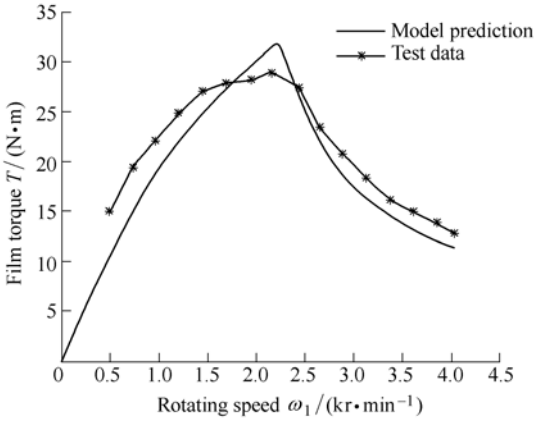

Fig. 17. Comparison of film torque between model prediction and test data

5 Conclusions

Based on the Navier-Stokes equations and the continuity equation, a mathematical model of fluid torque caused by shear stress is proposed in cylindrical coordinate by taking the viscosity-temperature characteristic of fluid into account. After solution by iterative method, the radial speed distribution, tangential speed distribution, pressure distribution and theoretical flow rate are determined and analyzed. The model of film equivalent radius is introduced and the fluid torque by shear stress is calculated. The conclusions are as follows:

(1) Based on the experimental research and Navier-Stokes equations, taking the viscosity-temperature characteristic of the fluid into account, the film torque caused by shear stress may be predicted correctly by the equivalent radius model and mathematical model which is solved by iterative method. The theoretical result has good agreement with experimental data.

(2) When the rotating speed is low, the radial speed distribution and pressure distribution are dominated by the pressure difference. The clearance is filled and the film

torque increases with rotating speed. However, when the rotating speed reaches a certain value, the centrifugal force plays an important role in the speed and pressure distribution. The pressure is negative at the outer radius and the feeding flow rate is less than theoretical, so the film starts to shrink which make the film torque decrease sharply.

References

[1] YAN Qingdong, ZHANG Liandi, ZHAO Yuqin. *Structure and design of tank*[M]. Beijing: Beijing Institute of Technology Press, 2007. (in Chinese)

[2] MENG Qingrui. *Study on hydro-viscous drive speed regulating start and control technology*[D]. Xuzhou: China University of Mining and Technology, 2008. (in Chinese)

[3] WEI Chenguan, ZHAO Jiaxiang. *Technology of hydro-viscous drive*[M]. Beijing: Defence Industry Press, 1996. (in Chinese)

[4] CHEN Ning. *Theoretical and application researches on hydroviscous drive*[D]. Hangzhou: Zhejiang University, 2003. (in Chinese)

[5] ZHANG Zhigang. *Study on several working characteristics of wet clutch*[D]. Hangzhou: Zhejiang University, 2010. (in Chinese)

[6] CAI Dujing, WEI Chenguan. A study on the dynamic performance of hydroviscous drives[J]. *Journal of Beijing Institute of Technology*, 1992, 1(2): 111–121.

[7] XIE Fangwei, HOU Youfu. Oil film hydrodynamic load capacity of hydro-viscous drive with variable viscosity[J]. *Industrial Lubrication and Tribology*, 2011, 63(3): 210–215.

[8] HUANG Jiahai, QIU Minxiu, LIAO Lingling. Numerical simulation of flow field between frictional pairs in hydroviscous drive surface[J]. *Chinese Journal of Mechanical Egineering*, 2008, 21(3): 72–75.

[9] CHEN Zhi. *Study on the drag torque for wet clutch*[D]. Beijing: Beijing Institute of Technology, 2009. (in Chinese)

[10] HASHIMOTO H, WADA, S, MURAYAMA Y. The performance of a turbulent-lubricated sliding bearing subject to centrifugal effect[J]. *Trans. Jpn. Soc. Mech. Eng. Ser. C*, 1984, 49(446): 1 753–1 761. (in Japanese)

[11] KATO Y, MURASUGI T, HIRANO H, et al. Fuel economy improvement through tribological analysis of the wet clutches and brakes of an automatic transmission[J]. *Society of Automotive Engineers of Japan*, 1993, 16(12): 57–60.

[12] YUAN Yiqing, LIU Eysion, JAMES H, et al. An improved hydrodynamic model for open wet transmission clutches[J]. *ASME Trans. J. Fluids Eng.*, 2007, 129(3): 333–337.

[13] YUAN Shihua, GUO Kai, HU JiBin, et al. Study on aeration for disengaged wet clutches using a two-phase flow model[J]. *ASME Trans. J. Fluids Eng.*, 2010, 132(11): 111304 (1–6).

[14] HIRT C W, NICHOLS B D. Volume of fluid (vof) method for the dynamics of free boundaries[J]. *J. Comput. Phy.*, 1981, 39(1): 201–225.

[15] HU Jibin, PENG Zengxiong, YUAN Shihua. Drag torque prediction model for the wet clutches[J]. *Chinese Journal of Mechanical Engineerring*, 2009, 22(2): 238–243.

[16] YUAN Shihua, PENG Zengxiong, JING Congbo. Experimental research and mathematical model of drag torque in single-plate wet clutch[J]. *Chinese Journal of Mechanical Engineering*, 2011, 24(1): 91–97.

[17] XIE Fangwei. *Influence law of temperature field and deformed interface on hydro-viscous drive characteristics*[D]. Xuzhou: China University of Mining and Technology, 2010. (in Chinese)

[18] HONG Yue. *Study behavior of speeding wet clutch and fuzzy controller*[D]. Shanghai: Shanghai University, 2004. (in Chinese)

[19] HU Jibin, PENG Zengxiong, WEI Chao. Experimental research on drag torque for single-plate wet clutch[J]. *Trans. ASME, J. Tribol*., 2012, 134(2): 014502(1–6).

[20] RAZZAQUE M M, KATO T. Effcets of groove orientation on hydrodynamic behavior of wet clutch coolant films[J]. *Trans. ASME, J. Tribol.*, 1999, 121(2): 808–815.

[21] APHALE C R, CHO J H, SCHULTZ W W, et al. Modeling and parametric study of torque in open clutch plates[J]. *Trans. ASME, J. Tribol.*, 2006, 128(2): 422–430.

Biographical notes

CUI Hongwei, born in 1986, is currently a PhD candidate at *Beijing Institute of Technology, China*. He received his bachelor degree from *Beijing Institute of Technology, China*, in 2008. His research interests include the technology of vehicular transmission and viscous drive.
Tel: +86-10-68911914; E-mail: tcyr@bit.edu.cn

YAO Shouwen, born in 1971, is currently an associate professor at *Beijing Institute of Technology, China*. He received his PhD degree from *China Academy of Railway Sciences, China,* in 2000. His research interests include the technology of vehicular transmission, viscous drive, etc.
Tel: +86-10-68918498; E-mail: yshouwen@gmail.com

YAN Qingdong, born in 1964, is currently a professor at *Beijing Institute of Technology, China*. He received his PhD degree from *Beijing Institute of Technology, China,* in 1995. His research interests include the technology of vehicular transmission, hydraulic transmission, viscous drive, etc.
Tel: +86-10-68949096; E-mail: yanqd@bit.edu.cn

FENG Shanshan, born in 1989, is currently a master candidate at *Beijing Institute of Technology, China*.
E-mail: ssfbit@gmail.com

LIU Qian, born in 1989, is currently a graduate student at *Beijing Institute of Technology, China.*
E-mail: liuqian_bit@163.com